International Journal of Pure and Applied Mathematics
Volume 85 No. 1 2013, 45-67
ISSN: 1311-8080 (printed version); ISSN: 1314-3395 (on-line version)
url: http://www.ijpam.eu
doi: http://dx.doi.org/10.12732/ijpam.v85i1.5

SPHERICAL FOLDING TESSELLATIONS BY KITES AND ISOSCELES TRIANGLES II

Catarina P. Avelino[1], Altino F. Santos[2] §
[1,2]Department of Mathematics, UTAD
5001-801 Vila Real, PORTUGAL

Abstract: The classification of the dihedral folding tessellations of the sphere and the plane whose prototiles are a kite and an equilateral triangle were obtained in a recent paper, [1]. Concerning to isosceles triangles the classification is much harder, which is not surprising since more angles are involved. In this paper we extend this classification presenting all the dihedral folding tessellations of the sphere by kites and isosceles triangles in a particular case of adjacency. A list containing these tilings including its combinatorial structure is presentes in Table 1.

AMS Subject Classification: 52C20, 05B45, 52B05
Key Words: dihedral f-tilings, combinatorial properties, spherical trigonometry, symmetry groups

1. Introduction

By a *folding tessellation* or *folding tiling* of the sphere S^2 we mean an edge-to-edge pattern of spherical geodesic polygons that fills the whole sphere with no gaps and no overlaps, and such that the "underlying graph" has even valency at any vertex and the sums of alternate angles around each vertex are π.

Received: December 17, 2012

§Correspondence author

Folding tilings are strongly related to the theory of isometric foldings on Riemannian manifolds. In fact, the set of singularities of any isometric folding on a surface S corresponds to a folding tiling in S, see [11] for the foundations of this subject.

The study of these special class of tessellations was initiated in [3] with a complete classification of all spherical monohedral folding tilings (by congruent triangles, necessarily). Ten years latter, Ueno and Agaoka [12] have established the complete classification of all triangular spherical monohedral tilings (without any restriction on angles).

Dawson and Doyle have also been interested in special classes of spherical tilings, see [8], [9] and [10], for instance.

The complete classification of all spherical folding tilings by rhombi and triangles was obtained in 2005 [6]. A detailed study of the triangular spherical folding tilings by equilateral and isosceles triangles is presented in [7].

Spherical f-filings by two non congruent classes of isosceles triangles have recently obtained, [4].

Here we discuss dihedral folding tessellations by spherical kites and isosceles spherical triangles.

A spherical kite K (Figure 1(a)) is a spherical quadrangle with two congruent pairs of adjacent sides, but distinct from each other. Let us denote by $(\alpha_1, \alpha_2, \alpha_1, \alpha_3)$, $\alpha_2 > \alpha_3$, the internal angles of K in cyclic order. The length sides are denoted by a and b, with $a < b$. From now on T denotes a spherical isosceles triangle with internal angles β and γ ($\gamma \neq \beta$), and length sides c and d, see Figure 1(b).

We shall denote by $\Omega(K, T)$ the set, up to isomorphism, of all dihedral folding tilings of S^2 whose prototiles are K and T.

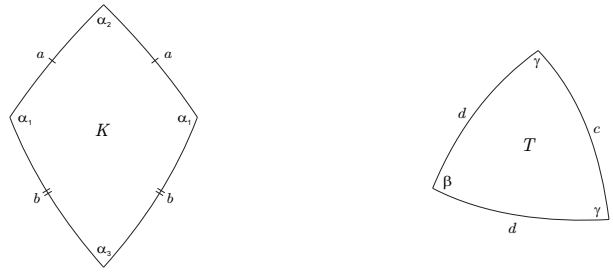

(a) (b)

Figure 1: A spherical kite and a spherical isosceles triangle

Taking into account the area of the prototiles K and T we have

$$2\alpha_1 + \alpha_2 + \alpha_3 > 2\pi \quad \text{and} \quad \beta + 2\gamma > \pi.$$

As $\alpha_2 > \alpha_3$ we also have

$$\alpha_1 + \alpha_2 > \pi.$$

We begin by pointing out that any element of $\Omega(K, T)$ has at least two cells congruent to K and T, respectively, such that they are in adjacent positions and in one and only one of the situations illustrated in Figure 2.

After certain initial assumptions are made, it is usually possible to deduce sequentially the nature and orientation of most of the other tiles. Eventually, either a complete tiling or an impossible configuration proving that the hypothetical tiling fails to exist is reached. In the diagrams that follow, the order in which these deductions can be made is indicated by the numbering of the tiles. For $j \geq 2$, the location of tiling j can be deduced directly from the configurations of tiles $(1, 2, \ldots, j-1)$ and from the hypothesis that the configuration is part of a complete tiling, except where otherwise indicated.

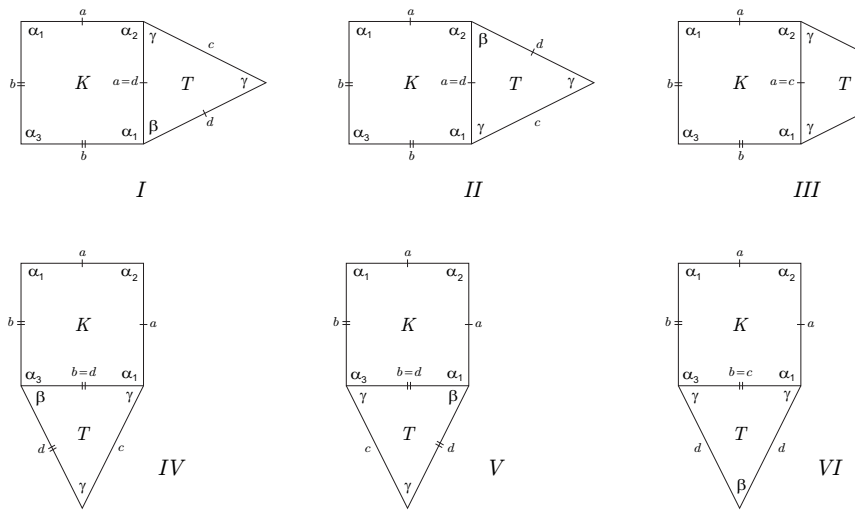

Figure 2: Distinct cases of adjacency

The first case has already been analyzed, [2]. In this paper we will consider the second case of adjacency. Our aim is to obtain all the dihedral f-tilings by kites and isosceles triangles. After the analysis of the cases of adjacency I and II, we believe that the study of the remaining cases will be handled more

briefly, since there is no more need to consider two adjacent tiles accordingly to the first two cases of adjacency.

2. Case of Adjacency II

Suppose that any element of $\Omega(K,T)$ has at least two cells congruent, respectively, to K and T, such that they are in adjacent positions as illustrated in Figure 2–II. As $a = d$, using trigonometric formulas, we obtain

$$\frac{\cos\gamma\,(1+\cos\beta)}{\sin\gamma\sin\beta} = \frac{\cos\frac{\alpha_3}{2}+\cos\alpha_1\,\cos\frac{\alpha_2}{2}}{\sin\alpha_1\,\sin\frac{\alpha_2}{2}}. \tag{1}$$

Concerning the angles of the triangle T we have necessarily one of the following situations:

$$\gamma > \beta \quad \text{or} \quad \gamma < \beta.$$

In the following subsections we consider separately each one of these cases.

2.1. $\gamma > \beta$

As $\gamma > \beta$, we have $\gamma > \frac{\pi}{3}$ and $c < a = d < b$, and so $c \neq b$, which determines tile 3 (Figure 3). In the following proposition we prove that there are no f-tilings verifying such a condition.

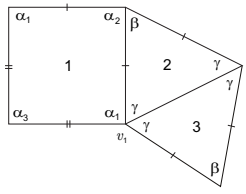

Figure 3: Local configuration

Proposition 1. *If $\gamma > \beta$, then $\Omega(K,T)$ is the empty set.*

Proof. Suppose that any element of $\Omega(K,T)$ has at least two cells congruent, respectively, to K and T, such that they are in adjacent positions as illustrated in Figure 2$-II$ (tiles 1 and 2 in Figure 3).

We begin distinguishing the cases $\alpha_1 \geq \alpha_2 > \alpha_3$ and $\alpha_2 > \alpha_1, \alpha_3$ (includes the cases $\alpha_2 > \alpha_1 \geq \alpha_3$ and $\alpha_2 > \alpha_3 > \alpha_1$).

1. Suppose firstly that $\alpha_1 \geq \alpha_2 > \alpha_3$ ($\alpha_1 > \frac{\pi}{2}$). As $\alpha_1 + \gamma \leq \pi$, it follows that $\gamma < \frac{\pi}{2} < \alpha_1$ and $\beta < \gamma < \alpha_2$. At vertex v_1 (Figure 3) we have necessarily $\alpha_1 + \gamma + k\alpha_3 = \pi$, with $k \geq 0$. Taking into account the edge lengths, the last configuration extends to the one that follows (Figure 4(a)).

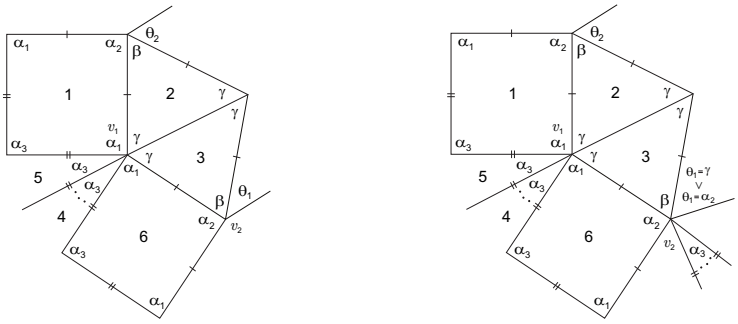

Figure 4: Local configurations

We have $\theta_1 \in \{\gamma, \alpha_2, \beta\}$.
If $\theta_1 \in \{\gamma, \alpha_2\}$ (Figure 4(b)) and

(i) $\alpha_2 + \theta_1 = \pi$, then $\beta + \rho = \pi$ has no solution;

(ii) $\alpha_2 + \theta_1 < \pi$, we have $\alpha_2 + \theta_1 + t\alpha_3 = \pi$, $t \geq 1$. Now, if $\theta_1 = \gamma$, at vertex v_2 arises an incompatibility on the sides; on the other hand, if $\theta_1 = \alpha_2$, the sum of alternate angles containing β must be of the form $\beta + \alpha_1 + (t-1)\alpha_3 + \alpha_1 > 2\alpha_1 > \pi$.

If $\theta_1 = \beta$ (Figure 5(a)), at vertex v_3 we get $\gamma + \gamma + \gamma > \pi$, which is a contradiction.

2. Suppose now that $\alpha_2 > \alpha_1, \alpha_3$ ($\alpha_2 > \frac{\pi}{2}$) (Figure 3).

If $\alpha_1 + \gamma = \pi$ (Figure 5(b)), we must have $\theta_1 = \beta$. Consequently, taking into account the edge lengths, at vertex v we obtain $\gamma + \gamma + \gamma > \pi$, which is not possible.

Therefore, $\alpha_1 + \gamma < \pi$. If $\alpha_1 \geq \gamma$ (see Figure 4(a)), we have $\theta_1 \in \{\gamma, \beta\}$. The analysis of both cases is analogous to the one made for 1.

Consequently, $\gamma > \alpha_1$ and, as $\alpha_1 + \gamma < \pi$, we also have $\alpha_1 < \frac{\pi}{2}$. Given the area of K, it follows that $\alpha_2 + \alpha_3 > \pi$, and so in a sum of alternate angles containing α_2 can exist only angles β (see Figure 6(a)). At vertex v it follows that $\gamma + \gamma \leq \pi$. Taking into account that β is the smallest angle and also

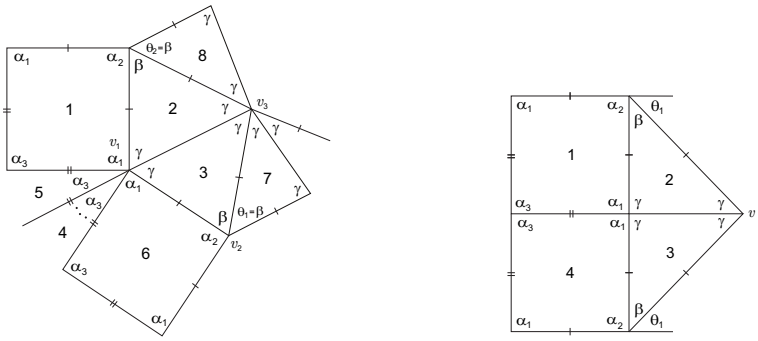

Figure 5: Local configurations

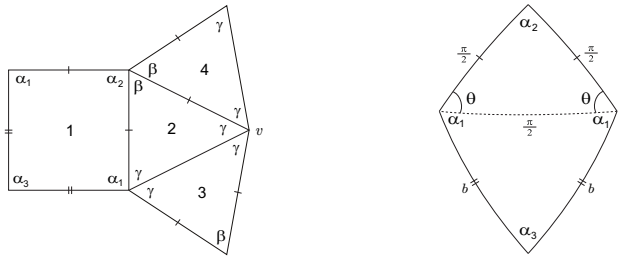

Figure 6: Local configurations

$2\gamma + \beta > \pi$, we conclude that $\gamma + \gamma = \pi$ and so $a = \gamma = \frac{\pi}{2}$. Considering the kite K divided as shown in Figure 6(b), we obtain $\theta = \frac{\pi}{2}$. But then $\alpha_1 > \frac{\pi}{2}$, which is not possible. □

2.2. $\gamma < \beta$

As $\gamma < \beta$, we have $\beta > \frac{\pi}{3}$ and $a < b, c$. In the following propositions we consider separately each one of the following situations:

$$\alpha_1 \geq \alpha_2 > \alpha_3, \quad \alpha_2 > \alpha_1 \geq \alpha_3 \quad \text{and} \quad \alpha_2 > \alpha_3 > \alpha_1.$$

Proposition 2. *If $\alpha_1 \geq \alpha_2 > \alpha_3$, then $\Omega(K,T) \neq \emptyset$ iff*

(i) $\alpha_1 + \gamma = \pi$, $\alpha_2 = \beta = \frac{\pi}{2}$ *and* $\alpha_3 = \frac{\pi}{k}$, *with* $k \geq 3$ *and* $\gamma = \gamma_k = \arccos\left(\frac{\sqrt{2}}{2}\cos\frac{\pi}{2k}\right)$, *or*

(ii) $\alpha_1 + \gamma = \pi$, $\alpha_2 + \beta = \pi$ *and* $\gamma = \alpha_3 = \frac{\pi}{k}$, *with* $k \geq 3$ *and* $\beta = \beta_k = 2\arcsin\left(2\cos\frac{\pi}{2k} - \sec\frac{\pi}{2k}\right)$.

In the first case, for each $k \geq 3$, *there is a unique f-tiling denoted by* $\mathcal{E}^k$. *A planar representation of* $\mathcal{E}^k$ *is given in Figure 15(b). 3D representations for* $k = 3$ *and* $k = 4$ *are given in Figure 16.*

In the last situation there is a single f-tiling, $\mathcal{H}^k$, *for each* $k \geq 3$. *The corresponding planar and 3D representations, for* $k = 3$ *and* $k = 4$, *are given in Figure 20 and Figure 21, respectively.*

Proof. Suppose that any element of $\Omega(K,T)$ has at least two cells congruent, respectively, to K and T, such that they are in adjacent positions as illustrated in Figure $2-II$ and $\alpha_1 \geq \alpha_2 > \alpha_3$ ($\alpha_1 > \frac{\pi}{2}$). With the labeling of Figure 7(a), at vertex v_1 we have

$$\theta_1 = \alpha_1, \quad \theta_1 = \beta \quad \text{or} \quad \theta_1 = \alpha_2.$$

Note that $\theta_1 \neq \gamma$, as the case of adjacency I analyzed in [2] (Proposition 2.3),

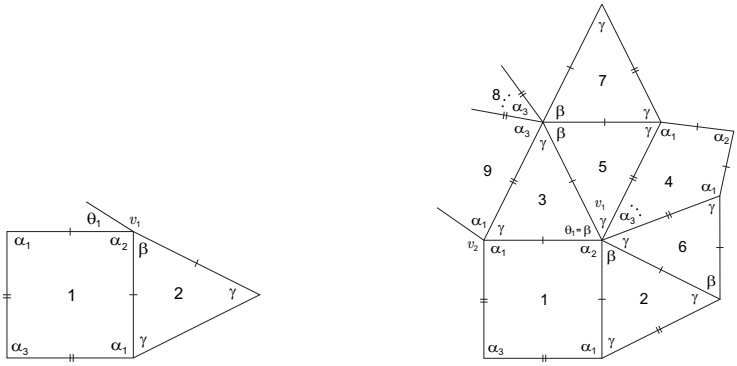

Figure 7: Local configurations

give not rise to any f-tiling.

1. Suppose firstly that $\theta_1 = \alpha_1$. We have $\alpha_1 + \beta \leq \pi$ ($\beta < \frac{\pi}{2} < \alpha_1$), and so at vertex v_1 we must have $\alpha_1 + \beta + k\alpha_3 = \pi$, with $k \geq 0$. It follows that the other sum of alternate angles containing α_2 must be of the form $\alpha_2 + k\alpha_3 + \rho = \pi$, with $\rho \in \{\alpha_1, \gamma\}$. Nevertheless, each choice for ρ results in a contradiction.

2. Suppose now that $\theta_1 = \beta$. We consider separately the cases $\beta + \beta < \pi$ and $\beta + \beta = \pi$.

2.1 If $\beta + \beta < \pi$, i.e. $\beta < \frac{\pi}{2}$, then $\beta + \beta + k_1\alpha_2 + k_2\alpha_3 = \pi$, with $k_1, k_2 \geq 0$ and $k_1 + k_2 > 0$.

If $k_1 \neq 0$, then $\alpha_1 > \beta > \gamma > \alpha_2 > \alpha_3$. As the set of vertices of valency four must be nonempty, $\alpha_1+\alpha_2 > \pi$ and $2\beta+\gamma > \pi$, we have necessarily $\alpha_1+\alpha_3 = \pi$. Taking into account the edge lengths, we get $\alpha_1 + \alpha_3 = \pi = \gamma + \alpha_3$, and so $\alpha_1 = \gamma$, which is not possible.

Thus, $k_1 = 0$, i.e., $\beta + \beta + k_2\alpha_3 = \pi$, $k_2 \geq 1$. The last configuration is extended to the one illustrated in Figure 7(b). The other sum of alternate angles at vertex v_1 must be $\alpha_2+\gamma+(k-1)\alpha_3+\gamma = \pi$, and so $\beta > \alpha_2$ (implying tile 7 and $\alpha_2 > \gamma$). But an impossibility arises at vertex v_2 as $\alpha_1 + \alpha_1 > \pi$.

2.2 If $\beta + \beta = \pi$, then $\alpha_2 + \rho = \pi$, with $\rho \in \{\alpha_2, \beta\}$ (Figure 8(a)). In any case, we have $\alpha_2 = \beta = \frac{\pi}{2}$ and, observing Figure 8(b), we conclude that $K = T \cup T^{\mathbb{I}}$. Therefore, $\alpha_1 > \beta = \alpha_2 = \frac{\pi}{2} > \gamma, \alpha_3$, and $\gamma > \frac{\pi}{4}$. At vertex v_2 we have $\alpha_1 + k\alpha_3 = \pi$, $k \geq 1$, or $\alpha_1 + \gamma + t\alpha_3 = \pi$, $t \geq 0$. The first case leads

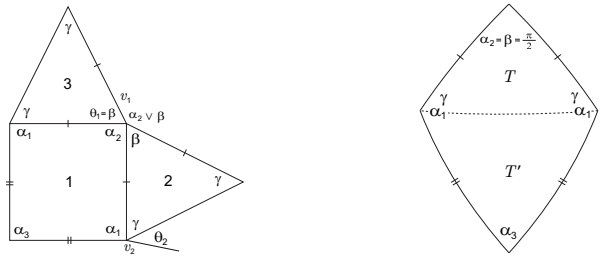

(a) (b)

Figure 8: Local configurations

to a contradiction, as the other sum of alternate angles at vertex v_2 must be $\gamma + k\alpha_3 = \pi$, $k \geq 1$, implying $\alpha_1 = \gamma$.

Thus, $\alpha_1 + \gamma + t\alpha_3 = \pi$, $t \geq 0$, and $\theta_2 = \alpha_3$ or $\theta_2 = \gamma$.

If $\theta_2 = \alpha_3$ (Figure 9(a)), and so $t > 0$, then, using similar arguments, at vertex v_3 we must have $\alpha_1 + \gamma + t\alpha_3 = \pi$. As we can observe in Figure 9(b), we reach a contradiction at vertex v_4.

Therefore we have $\theta_2 = \gamma$. Now, we distinguish the cases $\alpha_1 + \gamma < \pi$ and $\alpha_1 + \gamma = \pi$, i.e., $t > 0$ and $t = 0$.

The first case leads to $\alpha_1+\gamma+t\alpha_3 = \pi$, $t > 0$ (see Figure 10(a)). Note that tile 5 follows, by symmetry, the same analysis applied to tile 4. At vertex v_3 it follows that $\alpha_1 + \alpha_1 > \pi$, which is a contradiction.

Then, $t = 0$ (see Figure 10(b)), and $\theta_3 \in \{\gamma, \beta, \alpha_2\}$. We now analyze each possible choice for θ_3.

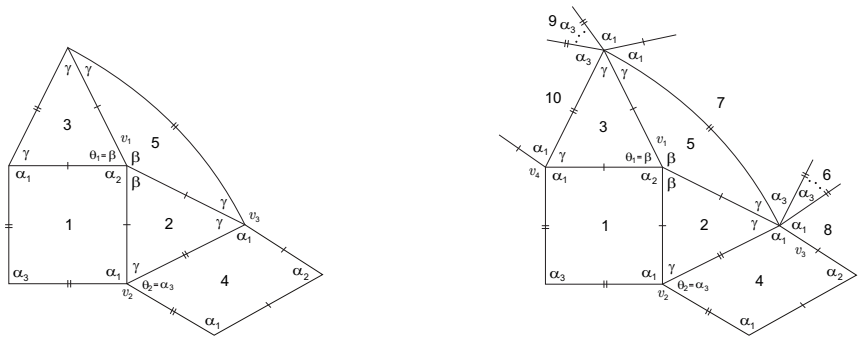

Figure 9: Local configurations

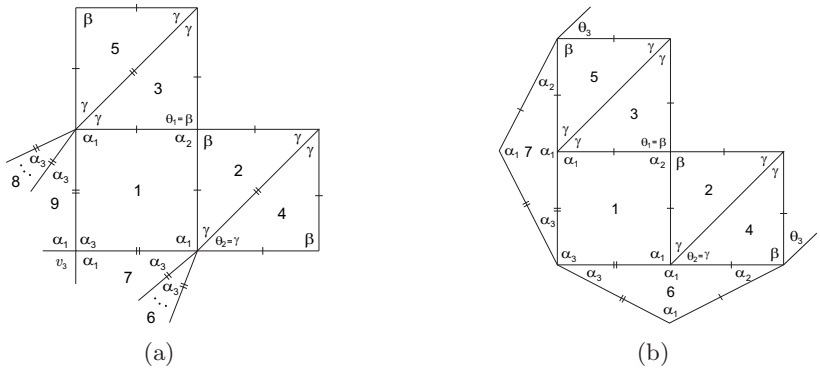

Figure 10: Local configurations

2.2.1 If $\theta_3 = \gamma$, the last configuration extends to the one illustrated in Figure 11(a). At vertex v_4 we obtain $\alpha_1 + \gamma = \pi = \beta + \alpha_3$, i.e., $\alpha_3 = \frac{\pi}{2}$, which is an absurd.

2.2.2 Suppose now that $\theta_3 = \beta$ (Figure 11(b)). If $\theta_4 = \alpha_3$, we get the configuration illustrated in Figure 12(a). But an incompatibility can not be avoided at vertex v_6 (note that the choice for tile 12 has analogous arguments to the ones used for tile 4).

Therefore, $\theta_4 = \gamma$, and so $\frac{\pi}{4} < \gamma \leq \frac{\pi}{3}$. If $\gamma = \frac{\pi}{3}$, we have $\alpha_1 = \frac{2\pi}{3} = \gamma + \gamma$ and the decomposition illustrated in Figure 12(b), $K = T \cup T^{\prime}$. It follows that $\alpha_3 > \frac{\pi}{3}$ (area of $T^{\prime} = K \setminus T$), and so $\alpha_3 + \alpha_3 + \rho = \pi$ is a condition that becomes impossible to be satisfied. Thus, $\gamma < \frac{\pi}{3}$ and $\gamma + \gamma + \gamma + k\alpha_3 = \pi$,

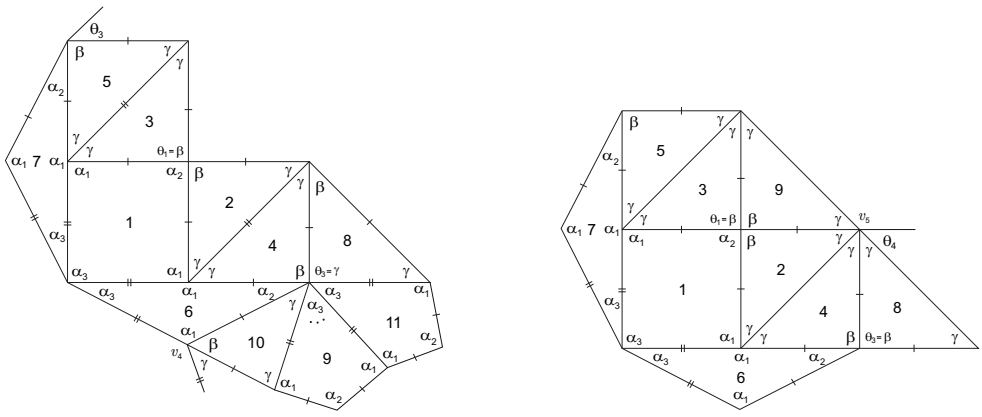

(a) (b)

Figure 11: Local configurations

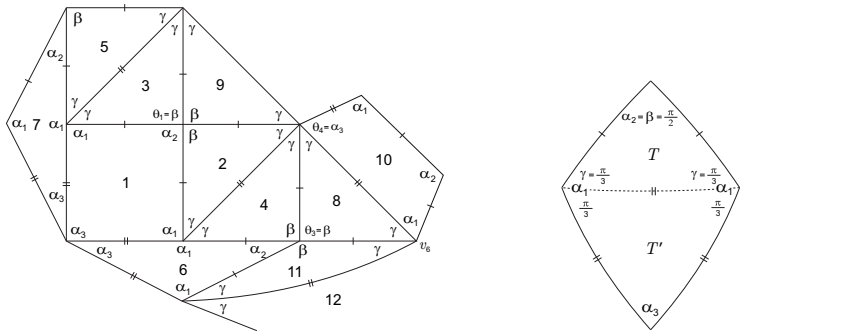

(a) (b)

Figure 12: Local configurations

$k \geq 1$. Nevertheless, in this case we also obtain a contradiction, see vertex v_6 in Figure 13(a).

2.2.3 Considering $\theta_3 = \alpha_2$, we obtain the configuration of Figure 13(b). Now, $\theta_4 = \alpha_2$ or $\theta_4 = \beta$.

2.2.3.1 If $\theta_4 = \alpha_2$, and

(i) $\theta_5 = \alpha_3$ (Figure 14(a)), at vertex v_7 we have $\alpha_1 + \gamma = \pi = \alpha_3 + \rho$, with $\rho \in \{\beta, \alpha_2\}$. But this implies $\alpha_3 = \frac{\pi}{2}$, which is not possible.

(ii) $\theta_5 = \gamma$ (Figure 14(b)), according to the edge lengths, it follows that $b = c$.

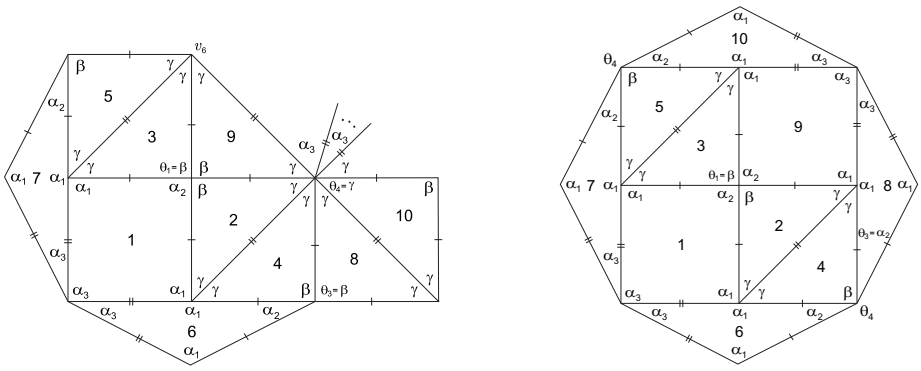

(a) (b)

Figure 13: Local configurations

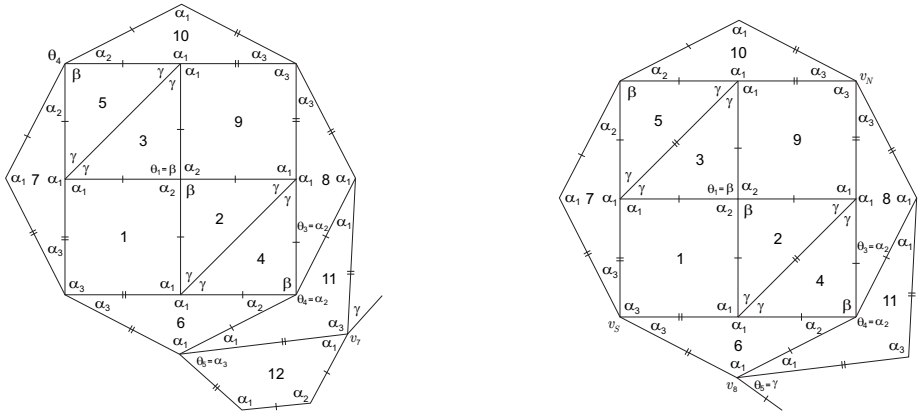

(a) (b)

Figure 14: Local configurations

As v_N and v_S are in antipodal positions, we conclude that $b = \frac{\pi}{3}$. Then, as $\cos b = \dfrac{\cos\beta + \cos^2\gamma}{\sin^2\gamma}$, we obtain $\gamma = \arctan\sqrt{2}$. Since $T^{\square}$ is an equilateral triangle (Figure 15(a)), we have $\alpha_1 - \gamma = \alpha_3$. Solving the system

$$\begin{cases} \alpha_1 + \gamma &= \pi \\ \alpha_1 - \gamma &= \alpha_3 \end{cases}$$

we get $\alpha_3 = \pi - 2\arctan\sqrt{2}$. At vertices v_N and v_S results that $\alpha_3 + \alpha_3 +$

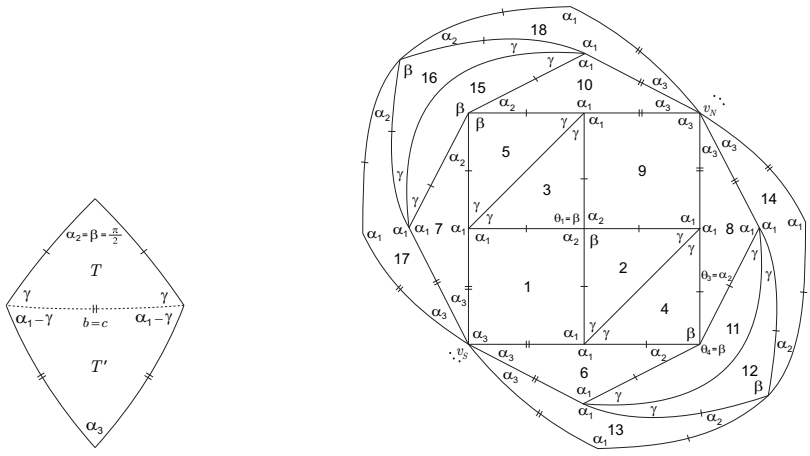

(a) (b) Planar representation of $\mathcal{E}^k$

Figure 15: Local configurations

$\rho > \pi$, for all $\rho \in \{\alpha_1, \alpha_2, \alpha_3, \beta, \gamma\}$.

2.2.3.2 In the case $\theta_4 = \beta$ the last configuration extends to the one illustrated in Figure 15(b). For each $k \geq 3$, there is a unique f-tiling denoted by $\mathcal{E}^k$. 3D representations of $\mathcal{E}^3$ and $\mathcal{E}^4$ are given in Figure 16.

From equation (1) one has $\gamma = \arccos\left(\frac{\sqrt{2}}{2}\cos\frac{\pi}{2k}\right)$.

3. Suppose finally that $\theta_1 = \alpha_2$ (Figure 7(a)).

3.1 If $\alpha_2 + \beta < \pi$ and

(i) $\alpha_2 \geq \gamma$, then $\alpha_2 + \beta + k\alpha_3 = \pi$, $k \geq 1$ (Figure 17(a)). As tiles 3 and 5 form the subcase analyzed in [2] (Proposition 2.3) within the case of the adjacency I, this local configuration will not give rise to any f-tiling.

(ii) $\gamma > \alpha_2$ (Figure 17(b)), it follows that $\alpha_1 + k\alpha_3 = \pi$, $k \geq 1$. The other sum of alternate angles must be of the form $\gamma + k\alpha_3 = \pi$, i.e., $\gamma = \alpha_1$, and so $\pi > \beta + \alpha_2 > \gamma + \alpha_2 = \alpha_1 + \alpha_2 > \pi$, which is a contradiction.

3.2 Suppose now that $\alpha_2 + \beta = \pi$ (Figure 18(a)). At vertex v_2 we have $\alpha_1 + k\alpha_3 = \pi$, $k \geq 1$, or $\alpha_1 + \gamma + t\alpha_3 = \pi$, $t \geq 0$. The first case leads to a contradiction, as we get $\alpha_1 = \gamma$.

Thus, $\alpha_1 + \gamma + t\alpha_3 = \pi$, $t \geq 0$. If $\theta_2 = \alpha_3$, and so $t > 0$ (Figure 18(b)), we reach a contradiction at vertex v_4.

Therefore, $\theta_2 = \gamma$ and we distinguish the cases $\alpha_1 + \gamma < \pi$ and $\alpha_1 + \gamma = \pi$, i.e., $t > 0$ and $t = 0$.

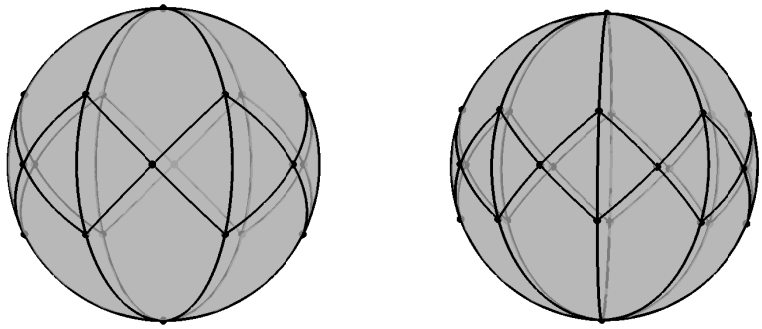

Figure 16: f-tilings $\mathcal{E}^k$, cases $k = 3$ and $k = 4$

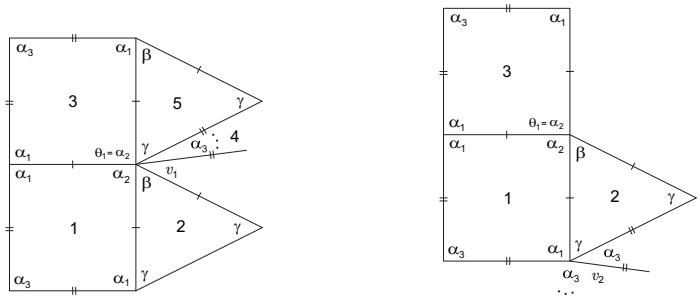

Figure 17: Local configurations

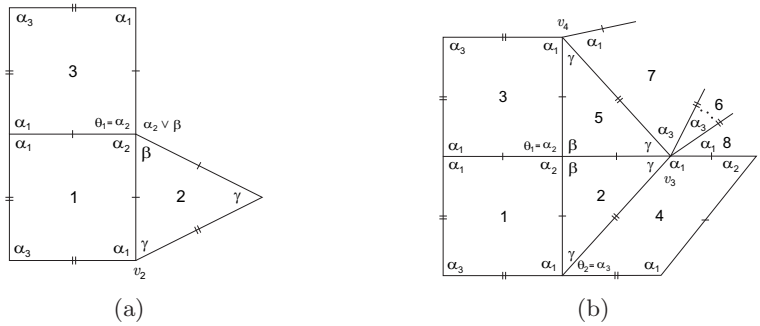

Figure 18: Local configurations

If $\alpha_1 + \gamma < \pi$, i.e., $\alpha_1 + \gamma + t\alpha_3 = \pi$, $t \geq 1$, then $\alpha_1 \geq \alpha_2 > \gamma > \alpha_3$ and $\alpha_1 > \beta > \gamma > \alpha_3$. We then obtain the configuration illustrated in

Figure 19(a). At vertex v_5 we have $\beta + \beta \leq \pi$. If $\beta + \beta < \pi$, we would

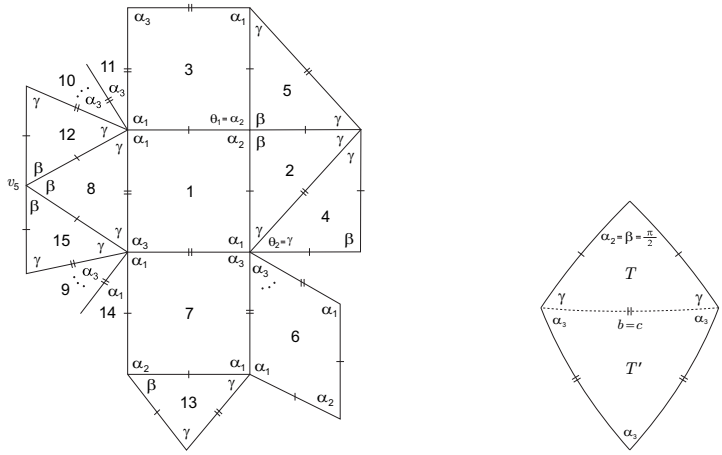

Figure 19: Local configurations

have $\beta + \beta + k\alpha_3 = \pi$, $k \geq 1$. But then the other sum of alternate angles is greater than π. Therefore, $\beta = \frac{\pi}{2} = \alpha_2$ and it follows that $\alpha_1 = \gamma + \alpha_3$ (see Figure 19(b)). Then, $\alpha_1 + \gamma + t\alpha_3 \geq \alpha_1 + \gamma + \alpha_3 = \alpha_1 + \alpha_1 > \pi$, which is not possible.

On the other hand, if $\alpha_1 + \gamma = \pi$ the last configuration extends to the one in Figure 20. Note that if $\alpha_1 + \alpha_3 < \pi$ at vertex v_1, taking into account the edge lengths, we get $\alpha_1 + \alpha_3 + \rho > \pi$, for all $\rho \in \{\alpha_1, \alpha_2, \beta, \gamma\}$. Also, if $\theta_2 = \gamma$ at vertex v_2, we would have $\alpha_1 + \gamma = \pi = \rho + \alpha_3$, with $\rho \in \{\alpha_2, \beta\}$, which is an absurd.

For each $k \geq 3$, we get a unique f-tiling denoted by $\mathcal{H}^k$. 3D representations for $k = 3$ and $k = 4$ are given in Figure 21.

Solving equation (1) with $\alpha_1 = \pi - \gamma$, $\alpha_2 = \pi - \beta$ and $\gamma = \alpha_3 = \frac{\pi}{k}$, we get

$$\frac{\cos\frac{\pi}{k}(1+\cos\beta)}{\sin\frac{\pi}{k}\sin\beta} = \frac{\cos\frac{\pi}{2k} - \cos\frac{\pi}{k}\sin\frac{\beta}{2}}{\sin\frac{\pi}{k}\cos\frac{\beta}{2}},$$

and so one has $\beta = 2\arcsin\left(2\cos\frac{\pi}{2k} - \sec\frac{\pi}{2k}\right)$. □

Proposition 3. *If $\alpha_2 > \alpha_1 \geq \alpha_3$, then $\Omega(K,T)$ is the empty set.*

Proof. Suppose that any element of $\Omega(K,T)$ has at least two cells congruent, respectively, to K and T, such that they are in adjacent positions as

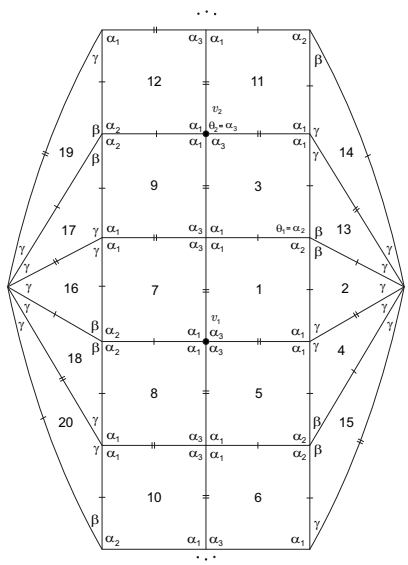

Figure 20: Planar representation of $\mathcal{H}^k$

illustrated in Figure 2$-II$ and $\alpha_2 > \alpha_1 \geq \alpha_3$ ($\alpha_2 > \frac{\pi}{2}$). With the labeling of Figure 22(a), we have

$$\theta_1 = \beta \quad \text{or} \quad \theta_1 = \gamma.$$

1. Suppose firstly that $\theta_1 = \beta$. We must have $\alpha_2 + \beta = \pi$, otherwise we get $\alpha_2 + \beta + k\alpha_3 = \pi = \beta + \rho + (k-1)\alpha_3 + \rho > \beta + 2\gamma > \pi$, with $k \geq 1$ and $\rho \in \{\alpha_1, \gamma\}$ (in this case we have $\alpha_2 > \frac{\pi}{2} > \beta$ and $\alpha_1 > \beta > \gamma$). Now we have $\theta_2 \in \{\alpha_1, \alpha_3, \gamma\}$ (Figure 22(b)).

1.1 If $\theta_2 = \alpha_1$, it follows that $\alpha_1 \leq \frac{\pi}{2}$. Taking into account the kite's area, we have $\alpha_2 + \alpha_3 > \pi$, and so $\alpha_3 > \beta$ ($\alpha_2 > \alpha_1 \geq \alpha_3 > \beta > \gamma$). If $\alpha_1 + \alpha_1 < \pi$, we get $\alpha_1 + \alpha_1 + \rho > \beta + 2\gamma > \pi$, for all $\rho \in \{\alpha_1, \alpha_2, \alpha_3, \beta, \gamma\}$. On the other hand, if $\alpha_1 + \alpha_1 = \pi$, we obtain $\gamma + \rho = \pi$, with $\rho \in \{\alpha_1, \gamma\}$, implying $\alpha_1 = \gamma$, which is also an absurd.

1.2 If $\theta_2 = \alpha_3$, then $\alpha_1 + \alpha_3 \leq \pi$. If $\alpha_3 \geq \beta$, then $\alpha_2 > \alpha_1 \geq \alpha_3 \geq \beta > \gamma$, and so $\alpha_1 + \alpha_3 < \alpha_2 + \beta = \pi$. But $\alpha_1 + \alpha_3 + \rho > \beta + 2\gamma > \pi$, for all $\rho \in \{\alpha_1, \alpha_2, \alpha_3, \beta, \gamma\}$. On the other hand, if $\beta > \alpha_3$, then $\alpha_2 + \alpha_3 < \alpha_2 + \beta = \pi$. Moreover, taking into account the kite's area, $\alpha_1 > \frac{\pi}{2} > \beta$ ($\alpha_2 > \alpha_1 > \frac{\pi}{2} > \beta > \gamma, \alpha_3$). Analyzing the configuration of Figure 23(a), at vertex v_2 we must have $\alpha_1 + \gamma + t\alpha_3 = \pi$, $t \geq 1$, leading to a contradiction at vertex v_3 ($\alpha_1 + \alpha_1 > \pi$).

1.3 We finally consider that $\theta_2 = \gamma$. We have $\alpha_1 + \gamma < \alpha_2 + \beta = \pi$. If $\alpha_3 \geq \beta$, then $\alpha_2 > \alpha_1 \geq \alpha_3 \geq \beta > \gamma$, and so $\alpha_1 + \gamma + \rho > \beta + 2\gamma > \pi$, for all

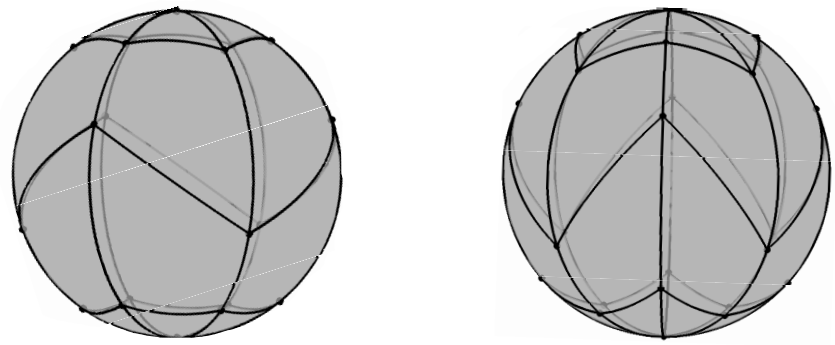

Figure 21: f-tilings $\mathcal{H}^k$, cases $k = 3$ and $k = 4$

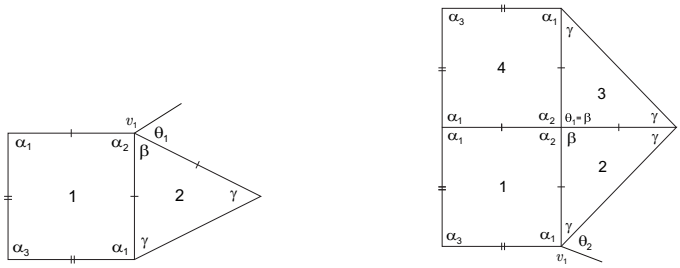

Figure 22: Local configurations

$\rho \in \{\alpha_1, \alpha_2, \alpha_3, \beta, \gamma\}$. On the other hand, if $\beta > \alpha_3$, then $\alpha_2 + \alpha_3 < \alpha_2 + \beta = \pi$. Therefore, $\alpha_1 > \frac{\pi}{2} > \beta$ ($\alpha_2 > \alpha_1 > \frac{\pi}{2} > \beta > \gamma, \alpha_3$). Analyzing the configuration of Figure 23(b), at vertices v_1 and v_1' we must have $\alpha_1 + \gamma + t\alpha_3 = \pi$, $t \geq 1$, and so $\alpha_2 > \alpha_1 > \frac{\pi}{2} > \beta > \gamma > \alpha_3$, $\gamma > \frac{\pi}{4}$. Nevertheless, we reach an incompatibility on the sides at vertex v_2.

2. Suppose now that $\theta_1 = \gamma$ (see Figure 22(a)). We distinguish the cases

$$\alpha_2 + \gamma < \pi \quad \text{and} \quad \alpha_2 + \gamma = \pi.$$

2.1 If $\alpha_2 + \gamma < \pi$ ($\gamma < \frac{\pi}{2} < \alpha_2$) and

(i) $\alpha_3 \geq \gamma$, then γ is the smallest angle and, as $\beta + 2\gamma > \pi$, v_1 must have valency four, which is an absurd.

(ii) $\gamma > \alpha_3$, we have $\alpha_2 > \alpha_1 > \gamma > \alpha_3$ and $\beta > \gamma > \alpha_3$. Moreover, $\alpha_1 > \frac{\pi}{2}$ since $\alpha_2 + \alpha_3 < \pi$.

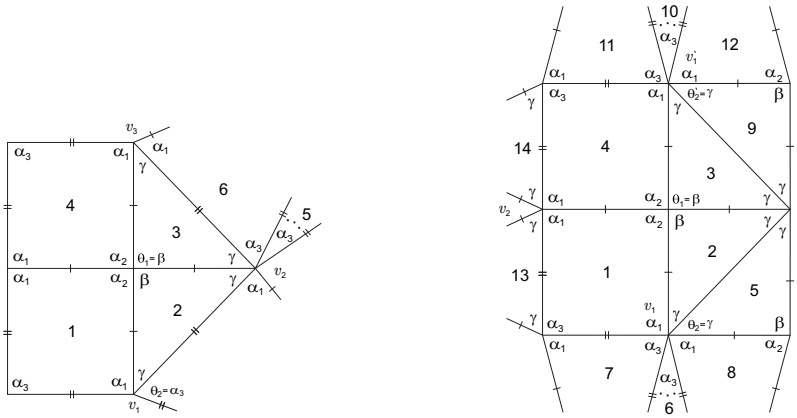

(a) (b)

Figure 23: Local configurations

(a) If $\beta \geq \alpha_2$, then $\beta \geq \alpha_2 > \alpha_1 > \frac{\pi}{2} > \gamma > \alpha_3$. As we always have vertices of valency four, we have $\beta + \gamma = \pi$ or $\beta + \alpha_3 = \pi$. But, taking into account the angles and edge lengths at vertex v_1, we have necessarily $\beta + \gamma + k\alpha_3 = \pi$, with $k \geq 1$, which is a contradiction.

(b) If $\alpha_2 > \beta$, at vertex v_1 we must have $\alpha_2 + \gamma + k\alpha_3 = \pi = \beta + \alpha_1 + k\alpha_3$, $k \geq 1$ (Figure 24(a)). Note that if $\theta_2 = \gamma$, we would have $\beta + \gamma + k\alpha_3 = \pi$, $k \geq 1$, implying $\beta = \alpha_2$, which is not possible. It follows that $\alpha_2 > \alpha_1 > \frac{\pi}{2} > \beta > \gamma > \frac{\pi}{4} > \alpha_3$. As the condition

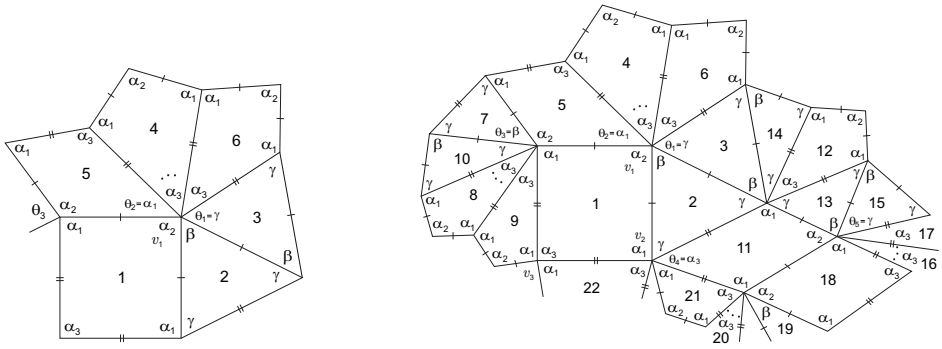

(a) (b)

Figure 24: Local configurations

$\theta_3 = \gamma$ originates two adjacent tiles from the case of the adjacency I ([2], Proposition 2.4), that in the case $\alpha_2 + \gamma < \pi$ give not rise to f-tilings, we conclude that $\theta_3 = \beta$ and the configuration extends to the one illustrated in Figure 24(b). Note that if $\theta_4 = \gamma$, at vertex v_2 we would have $\alpha_1 + \gamma + t\alpha_3 = \pi$, $t > k$, implying at vertex v_3 the condition $\alpha_1 + \alpha_1 > \pi$. The other possible choice for θ_4 is α_3, but in this case we also obtain a similar contradiction at vertex v_3. Note that after tile 12, we have $\gamma + \gamma + \gamma + (k-1)\alpha_3 = \pi$, $k \geq 1$, and the case $\theta_5 = \beta$ was already studied in 1, and no f-tilings were achieved.

2.2 If $\alpha_2 + \gamma = \pi$ (Figure 22(a)), we have $\beta + \rho = \pi$, with $\rho \in \{\gamma, \alpha_1\}$. The condition $\rho = \gamma$ gives rise to adjacent tiles of the adjacency case I, that, under these conditions, do not originate f-tilings ([2], Proposition 2.4). Therefore, $\rho = \alpha_1$ (Figure 25(a)). It follows that $\alpha_2 > \alpha_1, \beta$ and $\alpha_1, \beta > \gamma$. Now, $\theta_2 = \alpha_1$,

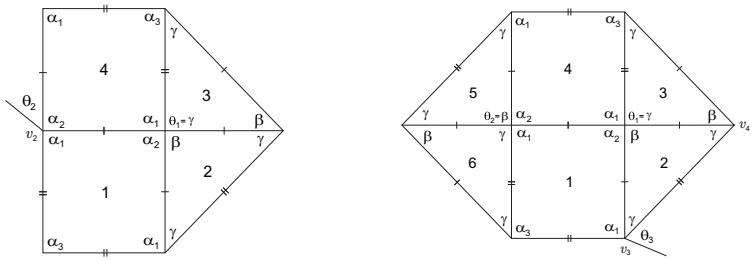

Figure 25: Local configurations

$\theta_2 = \gamma$ or $\theta_2 = \beta$.

2.2.1 If $\theta_2 = \alpha_1$, then $\alpha_1 \leq \frac{\pi}{2} \leq \beta$. Taking into account the kite's area, we have $\alpha_2 + \alpha_3 > \pi$, i.e., $\alpha_3 > \gamma$, implying that v_2 must have valency four $(\alpha_1, \alpha_2, \alpha_1, \gamma)$. But then an incompatibility on the sides arises at this vertex.

2.2.2 If $\theta_2 = \gamma$, we obtain adjacent tiles of the adjacency case I, that once again and under the current conditions, give not rise to f-tilings ([2], Proposition 2.4).

2.2.3 If $\theta_2 = \beta$, the last configuration extends to the one illustrated in Figure 25(b), and $\theta_3 \in \{\gamma, \alpha_1, \alpha_3\}$.

2.2.3.1 If $\theta_3 = \gamma$ and

(i) $\beta \geq \alpha_1$ $(\alpha_1 \leq \frac{\pi}{2})$, then $\alpha_2 + \alpha_3 > \pi$, and so $\alpha_3 > \gamma$. At vertex v_4 we get $\beta + \gamma < \alpha_2 + \gamma = \pi$. But $\beta + \rho_1 + \rho_2 > \pi$, for all $\rho \in \{\alpha_1, \alpha_2, \alpha_3, \beta, \gamma\}$.

(ii) $\alpha_1 > \beta$, then $\alpha_2 > \alpha_1 > \frac{\pi}{2} > \beta > \gamma > \frac{\pi}{4}$, and we obtain the configuration illustrated in Figure 26(a). At vertex v_5 we obtain a contradiction, as $\alpha_2 + \beta > \pi$.

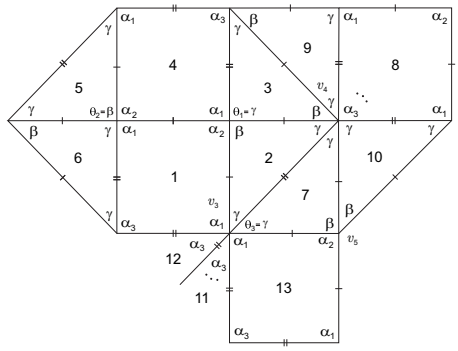

(a)

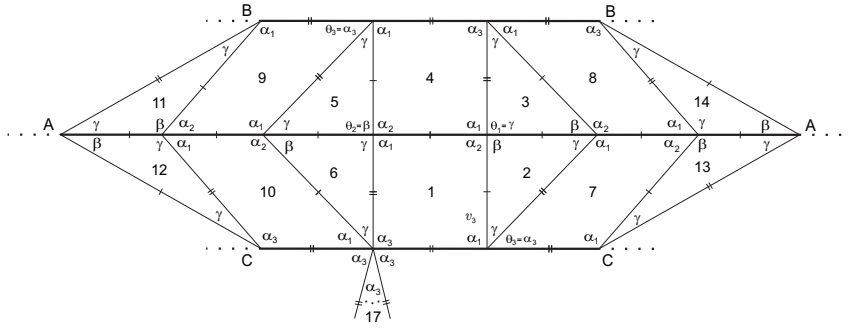

(b)

Figure 26: Local configurations

2.2.3.2 If $\theta_3 = \alpha_1$ (Figure 25(b)), it follows that $\alpha_1 \leq \frac{\pi}{2}$. By the kite's area, we obtain $\alpha_3 > \gamma$ and $\alpha_2 > \beta \geq \frac{\pi}{2} \geq \alpha_1 \geq \alpha_3 > \gamma$. Consequently, at vertex v_4 we have $\beta + \alpha_3 = \pi$, as $\beta + \alpha_3 + \rho > \pi$, for all $\rho \in \{\alpha_1, \alpha_2, \alpha_3, \beta, \gamma\}$. Nevertheless, there is no way to satisfy the angle-folding relation around this vertex.

2.2.3.3 If $\theta_3 = \alpha_3$, we obtain the configuration illustrated in Figure 26(b). Extending this configuration, the polygonal lines A, B and C close on themselves. Below the polygonal line B exists a great circle, and so $\alpha_1 + \gamma + \alpha_3 > \pi$. In fact, let R be the region below line B, n the number of sides of length b and $\alpha = \alpha_1 + \gamma + \alpha_3$. Thus, $n\alpha - (n-2)\pi > 2\pi$, implying $\alpha > \pi$.

Now, we have $\alpha_1 + \alpha_3 < \pi$ (see edge lengths), and so $\alpha_1 + t\alpha_3 = \pi$, with $t \geq 2$. Given the edge lengths, it also follows that $\gamma + t\alpha_3 = \pi$. But then $\gamma = \alpha_1$, which is an absurd. □

Proposition 4. *If $\alpha_2 > \alpha_3 > \alpha_1$, then $\Omega(K,T)$ is the empty set.*

Proof. Suppose that any element of $\Omega\,(K,T)$ has at least two cells congruent, respectively, to K and T, such that they are in adjacent positions as illustrated in Figure 2$-II$ and $\alpha_2 > \alpha_3 > \alpha_1$. With the labeling of Figure 27(a), we have

$$\theta_1 = \beta \quad \text{or} \quad \theta_1 = \gamma.$$

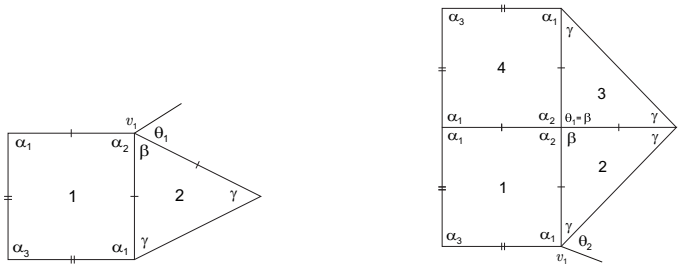

(a) (b)

Figure 27: Local configurations

1. Suppose firstly that $\theta_1 = \beta$. In this case $\alpha_2 + \beta \leq \pi$ and $\alpha_2 > \alpha_3 > \alpha_1 > \beta > \gamma$. As $\beta + 2\gamma > \pi$, it follows that $\alpha_2 + \beta = \pi$ (Figure 27(b)). θ_2 can be γ, α_3 or α_1. All these cases lead to a contradiction as

(i) if $\theta_2 = \gamma$, then $\alpha_1 + \gamma < \alpha_2 + \beta = \pi$; nevertheless, $\alpha_1 + \gamma + \rho > \beta + 2\gamma > \pi$, for all $\rho \in \{\alpha_1, \alpha_2, \alpha_3, \beta, \gamma\}$.

(ii) if $\theta_2 = \alpha_3$, it follows that $\alpha_1 + \alpha_3 = \pi$; taking into account the angles and edge lengths, we reach a contradiction.

(iii) $\theta_2 = \alpha_1$ leads to $\alpha_1 + \alpha_1 = \pi = \gamma + \rho < \pi$, with $\rho \in \{\gamma, \alpha_1\}$.

2. Suppose finally that $\theta_1 = \gamma$. As $\alpha_2 + \gamma \leq \pi$, we conclude that $\alpha_2 > \alpha_3 > \alpha_1 > \gamma$.

2.1 If $\alpha_2 + \gamma < \pi$, then $\alpha_2 + k\gamma = \pi$, with $k \geq 2$. The other sum of alternate angles containing β is $\beta + \rho_1 + \rho_2 + \ldots \geq \beta + \gamma + \gamma > \pi$, for all $\rho_1, \rho_2 \in \{\alpha_1, \alpha_2, \alpha_3, \beta, \gamma\}$, which is an absurd.

2.2 Suppose now that $\alpha_2 + \gamma = \pi = \beta + \theta_2$, with $\theta_2 \in \{\gamma, \alpha_1\}$. If $\theta_2 = \gamma$ (Figure 28(a)), then $\beta = \alpha_2 > \alpha_3 > \alpha_1 > \gamma$. But there is no way to satisfy the angle-folding relation around vertex v_2. On the other hand, if $\theta_2 = \alpha_1$

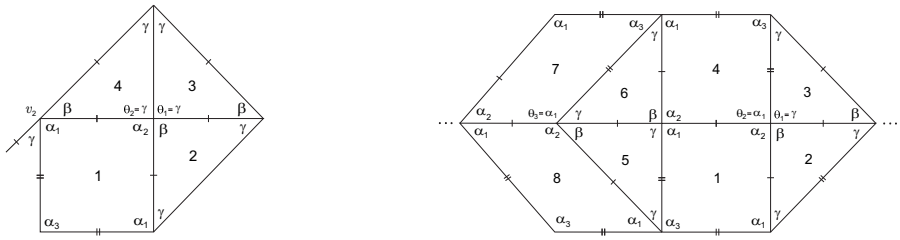

Figure 28: Local configurations

then $\alpha_2 > \beta > \gamma$ (Figure 28(b)). As $\beta + \rho_1 + \rho_2 > \beta + 2\gamma > \pi$, for all $\rho_1, \rho_2 \in \{\alpha_1, \alpha_2, \alpha_3, \beta, \gamma\}$, we get $\beta + \alpha_1 = \pi$ (tile 7). Consequently, $\alpha_1 + \alpha_3 \leq \pi$ and $\alpha_2 > \beta \geq \alpha_3 > \alpha_1 > \gamma$. Therefore, this case results analogous to the one studied in the previous proposition in 2.2.3.3. □

Concerning to the combinatorial structure of each tiling obtained, we have that

(i) any symmetry of $\mathcal{E}^k$, $k \geq 3$, fixes $N = (0, 0, 1)$ (and consequently $S = -N$) or maps N into S (and consequently S into N). The symmetries that fix N are generated, for instance, by the rotation $R^z_{\frac{\pi}{k}}$ (around the z axis) and the reflection ρ^{yz} (on the coordinate plane yoz), giving rise to a subgroup of $G(\mathcal{E}^k)$ isomorphic to D_{2k} (the dihedral group of order $4k$). Now, the map $\phi = \rho^{xy}$ is a symmetry of $\mathcal{E}^k$ that permutes N and S allowing us to get all the symmetries that map N into S. Now, since ϕ commutes with $R^z_{\frac{\pi}{k}}$ and ρ^{yz}, then it follows that $G(\mathcal{E}^k)$ is isomorphic to $C_2 \times D_{2k}$.

(ii) any symmetry of $\mathcal{H}^k$, $k \geq 3$, fixes N or maps N into S. The symmetries that fix N are generated, for instance, by the rotation $R^z_{\frac{2\pi}{k}}$ and the reflection ρ^{yz}, giving rise to a subgroup of $G(\mathcal{H}^k)$ isomorphic to D_k. The map $\phi = R^z_{\frac{\pi}{k}} \circ \rho^{xy} = \rho^{xy} \circ R^z_{\frac{\pi}{k}}$ is a symmetry of $\mathcal{H}^k$ that changes N and S. One has $\phi^{2k-1} \circ \rho^{yz} = \rho^{yz} \circ \phi$ and ϕ has order $2k$. It follows that ϕ and ρ^{yz} generate $G(\mathcal{H}^k)$. And so it is isomorphic to D_{2k}.

3. Summary

In Table 1 is shown a list of the spherical dihedral f-tilings whose prototiles are a spherical kite and an isosceles spherical triangle, K and T, of internal angles $(\alpha_1, \alpha_2, \alpha_1, \alpha_3)$, and (β, γ, γ), respectively, in case of adjacency II. Our notation is as follows:

- γ_0^k is the solution of equation (1), with $\alpha_2 = \beta = \frac{\pi}{2}$, $\alpha_1 = \pi - \gamma_0^k$ and $\alpha_3 = \frac{\pi}{k}$, with $k \geq 3$; β_1^k is the solution of equation (1), with $\alpha_2 = \pi - \beta_1^k$, $\alpha_1 = \pi - \gamma$ and $\gamma = \alpha_3 = \frac{\pi}{k}$, with $k \geq 3$.
- $|V|$ is the number of distinct classes of congruent vertices;
- N_1 and N_2 are, respectively, the number of triangles congruent to K and T, respectively, used in the dihedral f-tilings.
- $G(\tau)$ is the symmetry group of each tiling $\tau \in \Omega(K, T)$.

f-tiling	$\boldsymbol{\alpha_1}$	$\boldsymbol{\alpha_2}$	$\boldsymbol{\alpha_3}$	$\boldsymbol{\beta}$	$\boldsymbol{\gamma}$	$\lvert V\rvert$	N_1	N_2	$G(\tau)$
$\boldsymbol{\mathcal{E}^k}$, $\boldsymbol{k \geq 3}$	$\pi - \gamma_0^k$	$\frac{\pi}{2}$	$\frac{\pi}{k}$	$\frac{\pi}{2}$	γ_0^k	3	$4k$	$4k$	$C_2 \times D_{2k}$
$\boldsymbol{\mathcal{H}^k}$, $\boldsymbol{k \geq 3}$	$\pi - \gamma$	$\pi - \beta_1^k$	$\frac{\pi}{k}$	β_1^k	$\frac{\pi}{k}$	4	$4k$	$4k$	D_{2k}

Table 1: Combinatorial structure of dihedral f–tilings of S^2 by spherical kites and isosceles triangles in case of adjacency II

Acknowledgments

The authors acknowledge the financial support from the Portuguese Government through the FCT – Fundação para a Ciência e a Tecnologia, project PEst-OE/MAT/UI4080/2011.

References

[1] C.P. Avelino, A.F. Santos, Spherical and planar folding tessellations by kites and equilateral triangles, *Australasian Journal of Combinatorics*, **53** (2012), 109-125.

[2] C.P. Avelino, A.F. Santos, Spherical folding tessellations by kites and isosceles triangles: a case of adjacency, submitted.

[3] A.M. Breda, A class of tilings of S^2, *Geometriae Dedicata*, **44** (1992), 241-253.

[4] A.M. Breda, P.S. Ribeiro, Spherical f-tilings by two non congruent classes of isosceles triangles-I, *Mathematical Communicatins*, **17**, No. 1 (2012), 127-149.

[5] A.M. Breda, A.F. Santos, Dihedral f-tilings of the sphere by spherical triangles and equiangular well centered quadrangles, *Beiträge zur Algebra und Geometrie*, **45**, No. 2 (2004), 447-461.

[6] A.M. Breda, A.F. Santos, Dihedral f-tilings of the sphere by rhombi and triangles, *Discrete Mathematics and Theoretical Computer Science*, **7** (2005), 123-140.

[7] A.M. Breda, P.S. Ribeiro, A.F. Santos, A class of spherical dihedral f-tilings, *European Journal of Combinatorics*, **30**, No. 1 (2009), 119-132.

[8] R.J. Dawson, Tilings of the sphere with isosceles triangles, *Discrete and Computational Geometry*, **30** (2003), 467-487.

[9] R.J. Dawson, B. Doyle, Tilings of the sphere with right triangles I: the asymptotically right families, *Electronic Journal of Combinatorics*, **13**, No. 1 (2006), #R48.

[10] R.J. Dawson, B. Doyle, Tilings of the sphere with right triangles II: the $(1, 3, 2)$, $(0, 2, n)$ family, *Electronic Journal of Combinatorics*, **13**, No. 1 (2006), #R49.

[11] S.A. Robertson, Isometric folding of riemannian manifolds, *Proc. Royal Soc. Edinb. Sect. A*, **79** (1977), 275-284.

[12] Y. Ueno, Y. Agaoka, Classification of tilings of the 2-dimensional sphere by congruent triangles, *Hiroshima Mathematical Journal*, **32** (2002), 463-540.